Cement and Concrete Research 56 (2014) 29–39

Contents lists available at ScienceDirect

Cement and Concrete Research

journal homepage: http://ees.elsevier.com/CEMCON/default.asp

Mix design and properties assessment of Ultra-High Performance Fibre Reinforced Concrete (UHPFRC)

R. Yu *, P. Spiesz, H.J.H. Brouwers

Department of the Built Environment, Eindhoven University of Technology, P. O. Box 513, 5600 MB Eindhoven, The Netherlands

ARTICLE INFO

Article history:
Received 16 April 2013
Accepted 7 November 2013
Available online 26 November 2013

Keywords:
High-performance concrete (E)
Fibre reinforcement (E)
Mixture proportioning (A)
Low cement content

ABSTRACT

This paper addresses the mix design and properties assessment of Ultra-High Performance Fibre Reinforced Concrete (UHPFRC). The design of the concrete mixtures is based on the aim to achieve a densely compacted cementitious matrix, employing the modified Andreasen & Andersen particle packing model. One simple and efficient method for producing the UHPFRC is utilised in this study. The workability, air content, porosity, flexural and compressive strengths of the designed UHPFRC are measured and analyzed. The results show that by utilizing the improved packing model, it is possible to design UHPFRC with a relatively low binder amount. Additionally, the cement hydration degree of UHPFRC is calculated. The results show that, after 28 day of curing, there is still a large amount of unhydrated cement in the UHPFRC matrix, which could be further replaced by fillers to improve the workability and cost efficiency of UHPFRC.

1. Introduction

Ultra-High Performance Fibre Reinforced Concrete (UHPFRC) is a combination of high strength concrete and fibres. In particular, it is a super plasticised concrete, reinforced with fibres, with an improved homogeneity because traditional coarse aggregates are replaced with fine sand [1]. According to Richard and Cheyrezy [1], UHPFRC represents the highest development of High Performance Concrete (HPC) and its ultimate compressive strength depends on the curing conditions (either standard, steam or autoclave curing), possible thermal treatments as well as on the adopted manufacturing technique, and its value could rise up to 800 MPa in the case of compressive molding. For the production of UHPC or UHPFRC a large amount of cement is normally used. For instance, Rossi [2] presented an experimental study of the mechanical behaviour of an UHPFRC with 1050 kg/m^3 cement. Park [3] investigated the effects of hybrid fibres on the tensile behaviour of Ultra-High Performance Hybrid Fibre Reinforced Concrete, in which about 1000 kg/m^3 of binder was used. Considering that the high cost of UHPFRC is a disadvantage that restricts its wider usage, some industrial by-products such as ground granulated blast-furnace slag (GGBS) and silica fume (SF), have been used as partial cement replacements. For example, El-Dieb [4] produced UHPFRC with about 900 kg/m^3 cement and 135 kg/m^3 silica fume. Tayeh [5] utilised about 770 kg/m^3 cement and 200 kg/m^3 silica fume to produce UHPFRC as a repair material. Hassan [6] show some mechanical investigation on UHPFRC with around 650 kg/m^3 cement, 420 kg/m^3 GGBS and 120 kg/m^3 silica fume. Additionally, some wastes materials are also included in the UHPC or UHPFRC production to reduce its cost. Tuan [7,8] investigated the possibility of using rice husk ash (RHA) to replace silica fume (SF) in producing UHPC. The experimental result shows that the compressive strength of UHPC incorporating RHA reaches more than 150 MPa. Yang [9] utilised recycled glass cullet and two types of local natural sand to replace the more expensive silica sand in UHPFRC. Nevertheless, the experimental results show that the use of recycled glass cullet (RGC) gives approximately 15% lowers performance, i.e. flexural strength, compressive strength and fracture energy.

As commonly known, the sector of building materials is the third-largest CO_2 emitting industrial sector world-wide, as well as in the European Union. The cement production is said to represent 7% of the total anthropogenic CO_2 emissions [10–12]. Hence, one of the key sustainability challenges for the next decades is to design and produce concrete with less clinker and inducing lower CO_2 emissions than traditional one, while providing the same reliability and better durability [13,14]. Considering the successful achievement on application of UHPFRC for rehabilitation of bridges since 1999 [15], the UHPFRC seems to be one of the candidates to reduce the global warming impact of construction materials. However, as shown before, when producing UHPC or UHPCRC, the cement or binder content is always relatively high (normally more than 1000 kg/m^3). Although some investigation show that it is possible to replace significant amounts of cement in UHPC mixes by limestone powder or fine quartz sand, while keeping the amount water added constant, without significantly decreasing the compressive strength [13,16], how to find a reasonable balance between the binder amount and the mechanical properties of UHPC or UHPFRC remains still an open question.

* Corresponding author. Tel.: +31 40 247 5469; fax: +31 40 243 8595.
E-mail address: r.yu@tue.nl (R. Yu).

0008-8846/$ – see front matter © 2013 Elsevier Ltd. All rights reserved.
http://dx.doi.org/10.1016/j.cemconres.2013.11.002

As already been accepted, an optimum packing of the granular ingredients of concrete is the key for a good and durable concrete (Brouwers [17], Hüsken [18] and Hunger [19]). Nevertheless, from the available literature, it can be found that the investigation of design or production of UHPFRC with an optimised particle packing is not sufficient [20–23]. In most cases, the recipes of UHPC or UHPFRC are given directly, without any detailed explanation or theoretical support. Hence, it can be predicted that a large amount of binders or other particles are not well utilised in UHPFRC.

Consequently, the objective of this study is to effectively design and produce UHPFRC with low cement amount. The design of the concrete mixtures is based on the aim to achieve a densely compacted cementitious matrix, employing the modified Andreasen & Andersen particle packing model. Fillers (limestone and quartz powder) are used to replace cement in the concrete. The focus of this study is also directed towards the properties evaluation of this designed concrete, including the fresh and hardened state behaviour. Additionally, the TG/DSC was further employed to evaluate the hydration degree of cement in UHPC paste.

2. Materials and methods

2.1. Materials

The cement used in this study is Ordinary Portland Cement (OPC) CEM I 52.5 R, provided by ENCI (the Netherlands). A polycarboxylic ether based superplasticiser (BASF) is used to adjust the workability of concrete. Limestone and quartz powder are used as fillers to replace cement. Two types of sand are used, one is normal sand with the fractions of 0–2 mm and the other one is a micro-sand with the fraction 0–1 mm (Graniet-Import Benelux, the Netherlands). One type of commercial micro-silica (powder) is selected as pozzolanic material. Short straight steel fibres (length of 13 mm and diameter of 0.2 mm) are employed to produce UHPFRC. The detailed information of used materials is summarised in Table 1 and Fig. 1.

2.2. Experimental methodology

2.2.1. Mix design of UHPFRC

For the design of mortars and concretes, several mix design tools are in use. Based on the properties of multimodal, discretely sized particles, De Larrard and Sedran [21,22] postulated different approaches to design concrete: the Linear Packing Density Model (LPDM), Solid Suspension Model (SSM) and Compressive Packing Model (CPM). Based on the model for multimodal suspensions, De Larrard and Sedran [21] developed the Linear Packing Density Model, composing multimodal particle mixtures. The functions of the LPDM are describing the interaction between size classes of the materials used. Due to the linear character of the LPDM, the model was improved by De Larrard and Sedran [21] by introducing the concept of virtual packing density. The virtual packing density is the maximum packing density which is only attainable if the particles are placed one by one. The improvements of the LPDM resulted in the Solid Suspension Model (SSM). In the further development of their model, De Larrard and Sedran [22], introduced the compaction index to the so-called Compressive Packing Model (CPM). The compaction index considers the difference between actual packing density and virtual packing density and characterises therefore the placing process. However, also the CPM still uses the packing of monosized classes to predict the packing of the composed mixture made up of different size classes. Fennis et al. [24] have developed a concrete mix design method based on the concepts of De Larrard and Sedran [21,22]. However, all these design methods are based on the packing fraction of individual components (cement, sand etc.) and their combinations, and therefore it is complicated to include very fine particles in these mix design tools, as it is difficult to determine the packing fraction of such very fine materials or their combinations. Another possibility for mix design is offered by an integral particle size distribution approach of continuously graded mixes, in which the extremely fine particles can be integrated with relatively lower effort, as detailed in the following.

Table 1
Information of materials used.

Materials	Type	Specific density (kg/m^3)
Cement	CEM I 52.5 R	3150
Filler-1	Limestone	2710
Filler-2	Quartz	2660
Fine sand	Microsand	2720
Coarse sand	Sand 0–2	2640
Silica fume	Micro-silica	2200
Superplasticiser	Polycarboxylate ether	1050
Fibre	Steel fibre	7800

First attempts describing an aimed composition of concrete mixtures, which generally consists of continuously graded ingredients, can be traced already back to 100 years ago. The fundamental work of Fuller and Thomsen [25] showed that the packing of concrete aggregates is affecting the properties of the produced concrete. They concluded that a geometric continuous grading of the aggregates in the composed concrete mixture can help to improve the concrete properties. Based on the investigation of Fuller and Thompson [25] and Andreasen and Andersen [26], a minimal porosity can be theoretically achieved by an optimal particle size distribution (PSD) of all the applied particle materials in the mix, as shown in Eq. (1).

$$P(D) = \left(\frac{D}{D_{\max}}\right)^q \tag{1}$$

where $P(D)$ is a fraction of the total solids being smaller than size D, D is the particle size (μm), $D_{\max}$ is the maximum particle size (μm) and q is the distribution modulus.

However, in Eq. (1), the minimum particle size is not incorporated, while in reality there must be a finite lower size limit. Hence, Funk and Dinger [27] proposed a modified model based on the Andreasen and Andersen Equation. In this study, all the concrete mixtures are designed based on this so-called modified Andreasen and Andersen model, which is shown as follows [27]:

$$P(D) = \frac{D^q - D^q_{\min}}{D^q_{\max} - D^q_{\min}} \tag{2}$$

where $D_{\min}$ is the minimum particle size (μm).

The modified Andreasen and Andersen packing model has already been successfully employed in optimisation algorithms for the design of normal density concrete [18–19] and lightweight concrete [28,29]. Different types of concrete can be designed using Eq. (2) by applying different value of the distribution modulus q, as it determines the proportion between the fine and coarse particles in the mixture. Higher values of the distribution modulus ($q > 0.5$) lead to coarse mixture, while lower values ($q < 0.25$) result in concrete mixes which are rich in fine particles [30]. Brouwers [17,31] demonstrated that theoretically a q value range of 0–0.28 would result in an optimal packing. Hunger [19] recommended using q in the range of 0.22–0.25 in the design of SCC. Hence, in this study, considering that a large amount of fine particles are utilised to produce the UHPFRC, the value of q is fixed at 0.23.

In this research, the modified Andreasen and Andersen model (Eq. (2)) acts as a target function for the optimisation of the composition of mixture of granular materials. The proportions of each individual material in the mix are adjusted until an optimum fit between the composed mix and the target curve is reached, using an optimisation algorithm based on the Least Squares Method (LSM), as presented in Eq. (3). When the deviation between the target curve and the composed

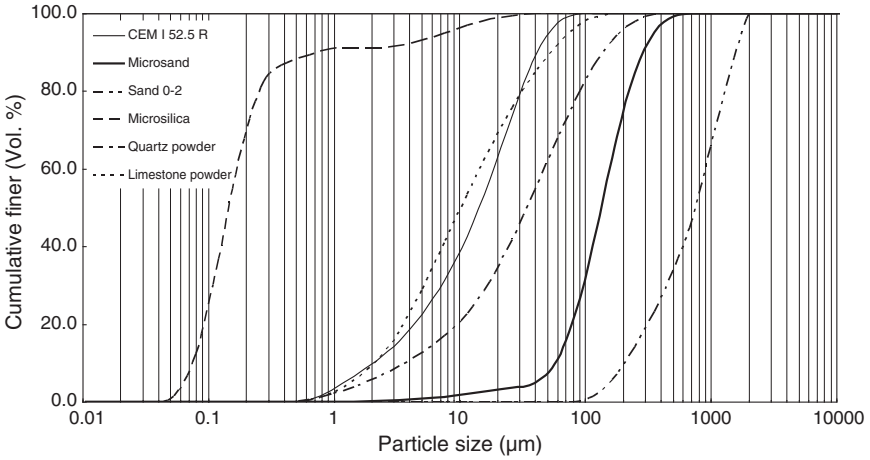

Fig. 1. Particle size distribution of the used materials.

mix, expressed by the sum of the squares of the residuals (RSS) at defined particle sizes, is minimised, the composition of the concrete is treated as the best one [18].

$$RSS = \sum_{i=1}^{n} \left(P_{mix}\left(D_i^{i+1}\right) - P_{tar}\left(D_i^{i+1}\right) \right)^2 \quad (3)$$

where P_{mix} is the composed mix, and the P_{tar} is the target grading calculated from Eq. (2).

Based on the optimised particle packing model, the developed UHPC mixtures are listed in Table 2. In total, three different types of UHPC composite are designed. The reference concrete mixture (UHPC1) has high cement content (about 875 kg/m^3). In UHPC2 and UHPC3, around 30% and 20% of cement is replaced by limestone and quartz powder, respectively. Although the raw material contents are different in each mixture, the particle packing of the UHPC1, UHPC2 and UHPC3 are very similar, which follows from the target curves and the resulting integral grading curves (Fig. 2). Hence, following the comparison of the properties of UHPC1, UHPC2 and UHPC3, it is possible to evaluate the efficiency of binders in UHPFRC and produce a dense UHPC matrix with a low binder content.

Additionally, for a normal fibre reinforced concrete, the fibre content is about 1–2% by volume of concrete [32]. However, in UHPFRC, this value increases to more than 2%, and sometime reaches even 5% [3]. Hence, in this study, to investigate the effect of fibres on the properties of UHPFRC, the steel fibres are added into the each UHPC mixes in the amount of 0.5%, 1.0%, 1.5%, 2.0% and 2.5% (by the volume of concrete), respectively. Due to the high complexity and the geometry of fibres, the effect of inclusion of steel fibres on the packing of concrete matrix is not considered in this study and will be investigated in the future.

Table 2
Recipes of developed UHPC.

Materials	UHPC1 (kg/m^3)	UHPC2 (kg/m^3)	UHPC3 (kg/m^3)
CEM I 52.5 R	874.9	612.4	699.9
Limestone	0	262.5	0
Quartz	0	0	175.0
Microsand	218.7	218.7	218.7
Sand 0–2	1054.7	1054.7	1054.7
Micro-silica	43.7	43.7	43.7
Water	202.1	202.1	202.1
Superplasticiser	45.9	45.9	45.9
Water/cement ratio	0.23	0.33	0.29

2.2.2. Employed mixing procedures

In this study, a simple and fast method is utilised to mix the UHPFRC. The detailed information of the mixing procedures is shown in Fig. 3. In total, 7 min and 30 s is required to finish the production of the UHPFRC, which is much shorter compared to some mixing procedures for UHPFRC [9,33]. Moreover, mixing is always executed under laboratory conditions with dried and tempered aggregates and powder materials. The room temperature while mixing, testing and concreting is constant at around 21 °C.

2.2.3. Workability of UHPFRC

To evaluate the workability of UHPFRC, the flow table tests are performed following EN 1015-3 [34]. From the test, two diameters perpendicular to each other (d_1 (mm) and d_2 (mm)) can be determined. Their mean is deployed to compute the relative slump (ξ_p) via:

$$\xi_p = \left(\frac{d_1 + d_2}{2d_0} \right)^2 - 1 \quad (4)$$

where d_0 represents the base diameter of the used cone (mm), 100 mm in case of the Hägermann cone. The relative slump ξ_p is a measure for the deformability of the mixture, which is originally introduced by Okamura and Ozawa [35] as the relative flow area R.

2.2.4. Air content in fresh UHPFRC

An alternative measure for the air content of UHPFRC is experimentally determined following the subsequent procedure. The fresh mixes are filled in cylindrical container of a known volume and vibrated for 30 s. The exact volume of the containers is determined beforehand using demineralised water at 20 °C. In order to avoid the generation of menisci at the water surface, the completely filled contained is covered with a glass plate, whose mass is determined before. Hence, based on the assumption that the fresh concrete is a homogeneous system, a possibility for determining the air content of concrete can be derived from the following equation:

$$\varphi_{air} = \frac{V_{container} - V_{solid} - V_{liquid}}{V_{container}} \quad (5)$$

where φ_{air} is the air content (%, V/V) of UHPFRC, $V_{container}$ is the volume of the cylindrical container that mentioned before, V_{solid} and V_{liquid} are the volumes of solid particles and liquid in the container (cm^3).

As the composition of each mixture is known, the mass percentage of each ingredient can be computed. Because it is easy to measure the total mass of concrete in the container, the individual masses of all

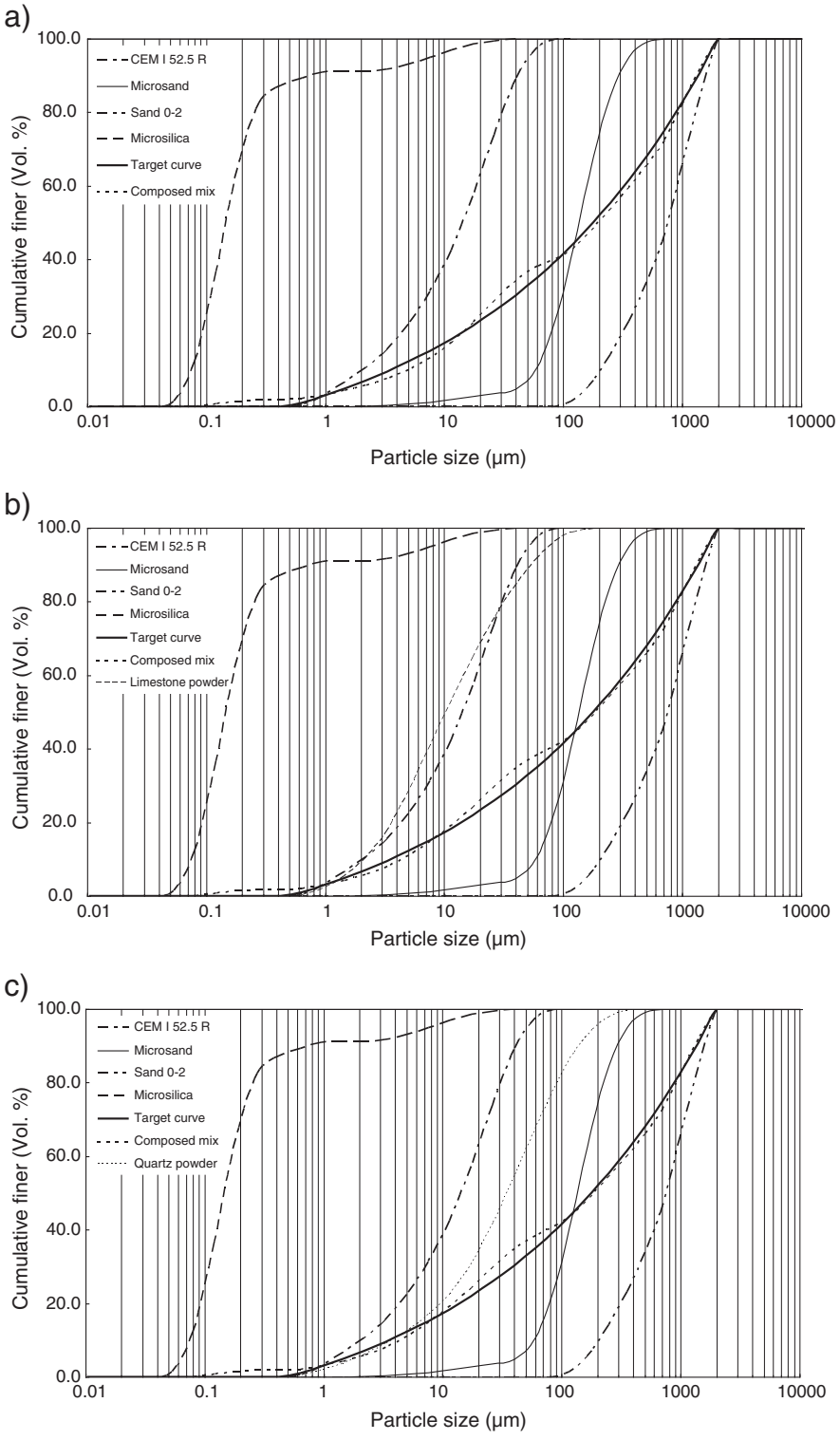

Fig. 2. PSDs of the involved ingredients, the target curve and the resulting integral grading line of the mixes UHPC1 (a), UHPC2 (b) and UHPC3 (c).

materials in the container can be obtained. Applying the density of the respective ingredients, the volume percentages of each mix constituent can be computed. Hence,

$$V_{solid} = \sum_i \frac{M_i}{\rho_i} \tag{6}$$

and

$$V_{liquid} = \sum_j \frac{M_j}{\rho_j} \tag{7}$$

where M_i and ρ_i are the mass (g) and density(g/cm^3) of the fraction i in solid materials, M_j and ρ_j are the mass(g) and density(g/cm^3) of the

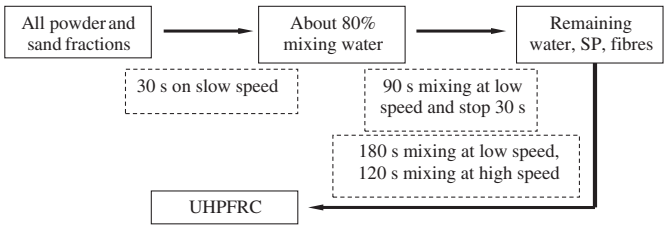

Fig. 3. Employed mixing procedure for producing UHPFRC.

fraction j in liquid materials, respectively. The schematic diagram for calculating the air content in concrete is shown in Fig. 4.

2.2.5. Mechanical properties of UHPFRC

After preforming the workability test, the UHPFRC is cast in molds with the size of 40 mm × 40 mm × 160 mm and compacted on a vibrating table. The prisms are demolded approximately 24 h after casting and then cured in water at about 21 °C. After curing for 7 and 28 days, the flexural and compressive strengths of the specimens are tested according to the EN 196-1 [36]. At least three specimens are tested at each age to compute the average strength.

2.2.6. Porosity of UHPFRC

The porosity of the designed UHPFRC is measured applying the vacuum-saturation technique, which is referred to as the most efficient saturation method [37]. The saturation is carried out on at least 3 samples (100 mm × 100 mm × 20 mm) for each mix, following the description given in NT Build 492 [38] and ASTM C1202 [39].

The water permeable porosity is calculated from the following equation:

$$\phi_{v,water} = \frac{m_s - m_d}{m_s - m_w} \cdot 100 \tag{8}$$

where $\phi_{v,water}$ is the water permeable porosity (%), m_s is the mass of the saturated sample in surface-dry condition measured in air (g), m_w is the mass of water-saturated sample in water (g) and m_d is the mass of oven dried sample (g).

2.2.7. Thermal test and analysis of UHPFRC

A Netzsch simultaneous analyzer, model STA 449 C, is used to obtain the Thermo-gravimetric (TG) and Differential Scanning Calorimetry (DSC) curves of UHPFRC paste. According to the recipes shown in Table 2, the pastes are produced without using any aggregates. Analyses were conducted at the heating rate of 10 °C/min from 20 °C to 1000 °C under flowing nitrogen.

Based on the TG test results, the hydration degree of the cement in each UHPFRC paste is calculated. Here, the loss-on-ignition (LOI) measurements of non-evaporable water content for hydrated UHPFRC paste are employed to estimate the hydration degree of cement [40].

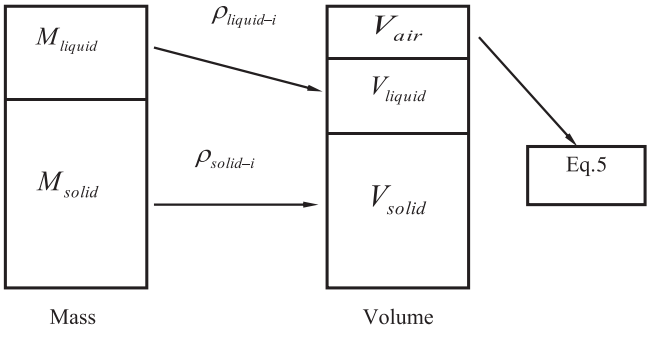

Fig. 4. Scheme of the method to estimate the air content in fresh UHPFRC.

Assuming that the UHPFRC paste is a homogeneous system, the non-evaporable water content is determined according to the following equation:

$$M'_{Water} = M_{105} - M_{1000} - M_{CaCO_3} \tag{9}$$

where the M'_{Water} is the mass of non-evaporable water (g), M_{105} is the mass of UHPC paste after heat treatment under 105 °C for 2 h (g), M_{1000} is the mass of UHPC paste after heat treatment under 1000 °C for 2 h (g), M_{CaCO_3} is the mass change of UHPC paste caused by the decomposition of $CaCO_3$ during the heating process (g). Then, the hydration degree of the cement in UHPFRC paste is calculated as:

$$\beta_t = \frac{M'_{Water}}{M_{Water-Full}} \tag{10}$$

where β_t is the cement hydration degree at hydration time t (%) and $M_{Water-Full}$ is the water required for the full hydration of cement (g). According to the investigation shown in [41], the maximum amount of non-evaporable water is 0.228 (g H_2O/g OPC) for a pure OPC system and 0.256 (g H_2O/g blended cement) for 90% OPC + 10% SF system. In this study, the cement is mixed with about 10% addition of micro-silica, hence the latter value is used in this study for the maximum ultimate bound water.

3. Experimental results and discussion

3.1. Relative slump flow ability of UHPFRC

The relative slump flow of fresh UHPFRC mixes, as described in Eq. (4), versus the volumetric content of steel fibres is depicted in Fig. 5. The data illustrates the direct relation between the additional steel fibres content and the workability of the fresh UHPFRC. It is important to notice that with the addition of steel fibres, the relative slump flow ability of all the UHPFRC linearly decreases. Especially the group of UHPC2, whose relative slump value sharply drops from 4.29 to 1.10, when the steel fibre content grows form 0.5% to 2.5% by volume of concrete. Moreover, with the same content of steel fibres, the relative slump of UHPC2 is always the largest, which is followed by UHPC3 and UHPC1, respectively. This difference between them is quite obvious at a low fibre amount and then gradually declines, when additional fibres are added. Furthermore, based on the linear equations (shown in Fig. 5), it can be noticed that the slope of the line for the UHPC2 is the largest, which means the addition of fibres can cause more notable workability loss of UHPC2.

As commonly known, the effect of steel fibres on the workability of concrete is mainly due to three following reasons [32]: 1) The shape of the fibres is much more elongated compared with aggregates and

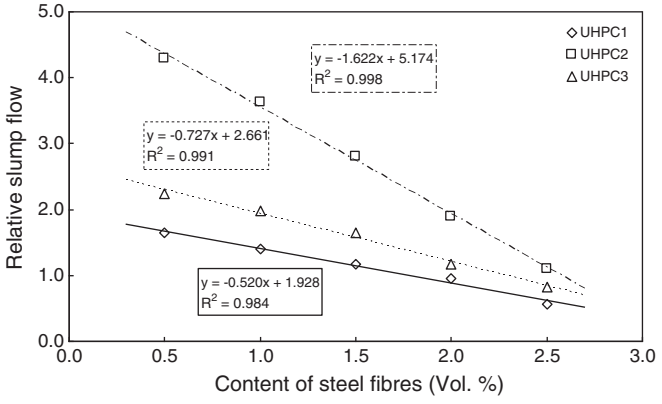

Fig. 5. Variation of the relative slump flow of UHPFRC with different cement content as function of steel fibre content.

the surface area at the same volume is higher, which can increase the cohesive forces between the fibres and matrix; 2) Stiff fibres change the structure of the granular skeleton, and stiff fibres push apart particles that are relatively large compared with the fibre length; 3) Steel fibres often are deformed (e.g. have hooked ends or are wave-shaped) to improve the anchorage between fibre and the surrounding matrix. The friction between hooked-end steel fibres and aggregates is higher compared with straight steel fibres. In this study, only short and straight steel fibres are used, which means the workability loss of concrete with the addition of fibres should be attributed to the increase in the internal surface area that produces higher cohesive forces between the fibres and concrete matrix. As presented by Edgington [42], with an increase of the fibre content, the workability of the normal concrete decreases sharply. Hence, it can be concluded that when more fibres are added, the cohesive forces are higher, and the relative slump flow of the UHPFRC will decrease. Furthermore, the difference of cement content in each UHPFRC should also be considered. The cement content of UHPC1, UHPC2 and UHPC3 is 875 kg/m^3, 612 kg/m^3 and 699 kg/m^3, respectively. Hence, with the same water and superplasticiser amount, utilizing fillers to replace cement can significantly improve the workability of concrete, similarly to the results shown in [43–45].

To summarise, due to the high cohesive forces between the fibres and concrete matrix, the addition of steel fibres will decrease the workability of UHPFRC. The linear decrease of the relative slump of UHPFRC with the increase of steel fibre content can be observed in this research. However, similarly to normal concrete, appropriate utilization of fillers to replace the cement could also be treated as an effective method to improve the workability of UHPFRC.

3.2. Air content and porosity analysis of UHPFRC

The determined air content of UHPFRC in fresh state and the porosity of UHPFRC in hardened state are presented in Figs. 6 and 7. As can be seen in Fig. 6, all the curves are very similar, which implies that the particle packing and void fraction of the designed UHPFRC are close to each other. Especially when the content of steel fibres increases to 2.5%, the difference in the air content between them is difficult to distinguish. Moreover, with an increase of the content of steel fibres, the air content of each UHPFRC parabolically increases, which means the more steel fibres are added, the more air will be entrained into the UHPFRC.

The influence of additional steel fibres on the air content of UHPFRC could be explained by the effect of fibres on the particle packing of concrete ingredients. As shown by Grünewald [32], due to the internal force between the fibres and aggregate (and/or fibres themselves), the packing density of concrete will significantly decrease with the addition of steel fibres. Hence, in this study, with the increase of the fibre content, a clear increase of air content in UHPFRC can be observed.

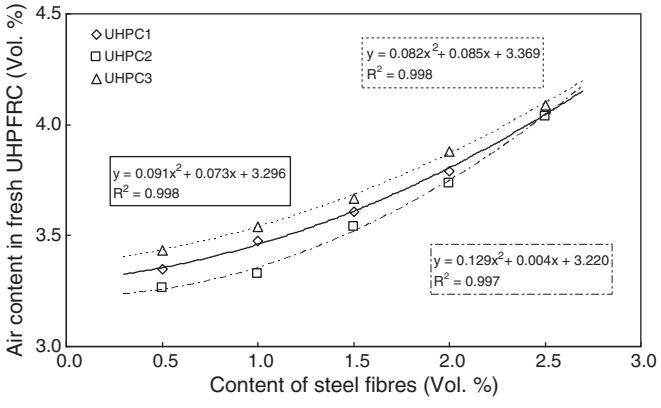

Fig. 6. Variation of the air content in fresh UHPFRC with different cement content as function of steel fibre content.

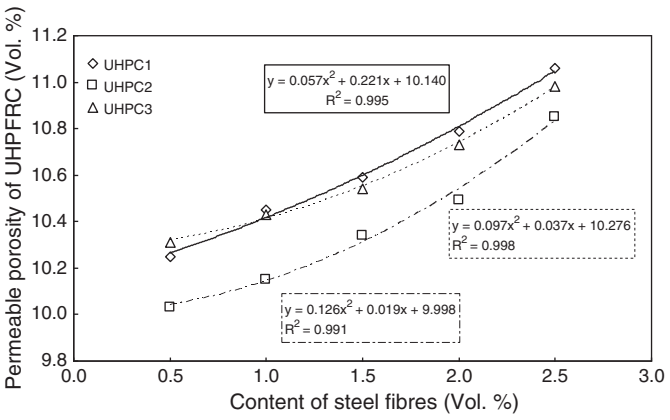

Fig. 7. Total water-permeable porosity of UHPFRC with different cement content as function of steel fibre content.

In Fig. 7, it can be noticed that the effect of steel fibres on porosity of concrete is similar to the effect of the steel fibres on the air content in fresh concrete (as shown in Fig. 6). With an increase of the content of steel fibres, the porosity of each developed UHPFRC parabolically grows. Moreover, the porosity values obtained in this study are smaller compared to conventional concrete. For instance, Safiuddin and Hearn [37] reported a porosity of 20.5% for concrete produced with a water/cement ratio of 0.60, employing the same measurement method (vacuum-saturation technique). Furthermore, with the same content of steel fibres, the porosity of UHPC2 is the smallest, while that the difference between UHPC1 and UHPC3 is small.

Here, assuming that the porosity of the UHPFRC is composed of the air voids (in fresh state concrete) and the paste porosity (generating during the hydration of cement). Hence, based on the results shown in Figs. 6 and 7, the paste porosity of UHPC mixes versus the volumetric steel fibres content is revealed in Fig. 8. It is apparent that with an increase of steel fibre content, the paste porosity remains relatively constant. For instance, in UHPC2, the paste porosity is in the range of 6.7–6.8%, while it increases to 6.8–6.9% and 6.9–7.0% for UHPC3 and UHPC1, respectively. According to the investigation of Tazawa [46], with the same water content, the more cement there is, the larger of the chemical shrinkage porosity of the hardened cement matrix will generate. Hence, the small difference of paste porosity between UHPC should also be owed to the different cement content.

To sum up, as supported by the experimental results, due to the optimised particle packing of concrete mixtures and low water/binder ratio, the designed UHPFRC has a low porosity and dense internal structure.

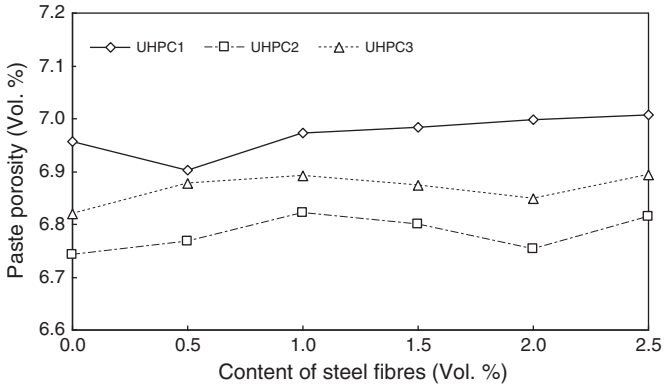

Fig. 8. Hardened paste porosity of UHPFRC with different cement and fibre content.

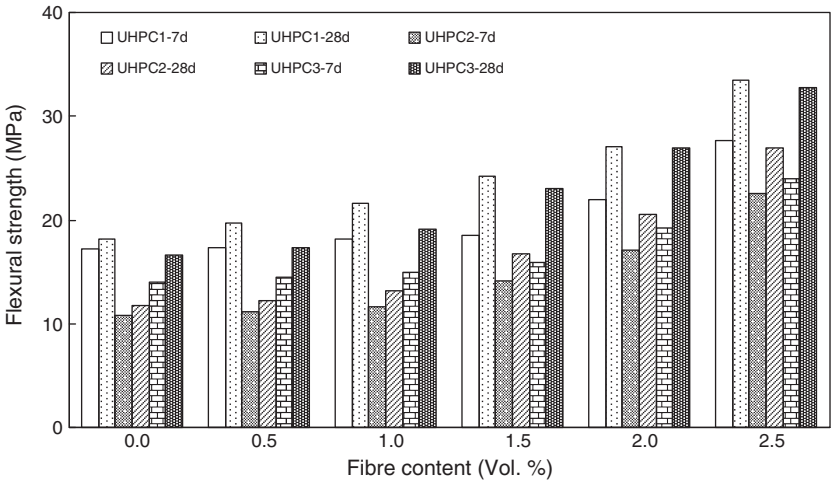

Fig. 9. Flexural strength of UHPFRC after curing for 7 and 28 days.

3.3. Mechanical properties analysis of UHPFRC

The flexural and compressive strengths of UHPFRC at 7 days and 28 days versus the volumetric steel fibres contents are shown in Figs. 9 and 10. It is important to notice that with the addition of steel fibres, the flexural and compressive strengths of UHPFRC can be significantly enhanced, similar as the results shown in [47–49]. Taking UHPC3 as an example, with the addition of steel fibres, the flexural strength at 28 days increases from 16.7 MPa to 32.7 MPa, and the compressive strength increases form 94.2 MPa and 148.6 MPa. Moreover, with the same fibre content and curing time, the flexural and compressive strengths of UHPC1 are always larger than those of UHPC2 and UHPC3. For instance, with the addition of 2.5% (by volume of concrete) steel fibres, the flexural and compressive strength of UHPC1 at 28 days are 33.5 MPa and 156 MPa, while that of UHPC2 are 27.0 MPa and 141.5 MPa, respectively. Additionally, the comparison of the binder amount and compressive strength (28 days) between the optimised and the non-optimised UHPFRC is shown in Table 3. It is clear that with lower binder amount, the compressive strength of the optimised UHPFRC is still comparable to the non-optimised UHPFRC (which have a large amount of binder). For instance, as the results shown by Hassan [6], about 1200 kg/m^3 of binder is utilised in producing UHPFRC, and its compressive strength at 28 days is about 150 MPa. However, in this study, there is only about 650 kg/m^3 of binders in UHPC2, but its compressive strength can also reach around 142 MPa. Hence, it can be concluded that, based on the modified Andreasen & Andersen particle packing model, it is possible to produce a UHPFRC with low binder amount.

Due to the addition of fibres, the fibres can bridge cracks and retard their propagation, which directly cause that the strength (especially the flexural strength) of concrete significantly increase. Additionally, the cement content also has a close relationship with the strength of concrete. As the investigation of Sun [50] show, with an increase of water/cement ratio, the interface between the matrix and aggregates or matrix and fibres will become denser. Hence, in this study, the UHPC1 (the one with the highest cement content) has the largest flexural and compressive strength, compared to that of UHPC2 and UHPC3. However, it should also be noticed that the strength difference between UHPC1 and UHPC3 is not so obvious anymore after 28 days, though that there is a 175 kg/m^3 difference in the content of cement between them. Consequently, the influence of steel fibres and cement content on the strength of UHPFRC should be considered separately.

To clarify the efficiency of the additional steel fibres on the flexural and compressive strengths of UHPFRC, the strength improvement ratio is utilised and shown as follows [51]:

$$K_t = \frac{S_i - S_0}{S_0} \ (i = 0.5, 1.0, 1.5, 2.0\ 2.5) \tag{11}$$

where K_t (%) is the strength improvement ratio, S_i (MPa) is the strength of concrete with fibres, i means the addition of fibres (by volume) and S_0 (MPa) is the strength of concrete without fibres.

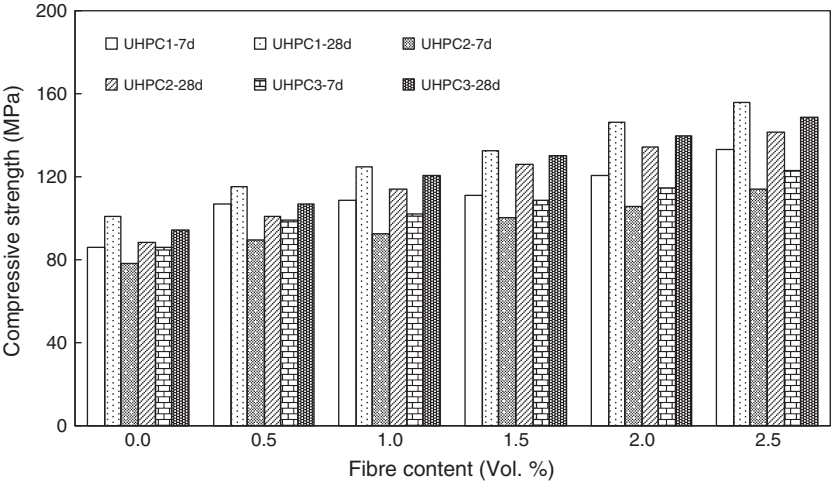

Fig. 10. Compressive strength of UHPFRC after curing for 7 and 28 days.

Table 3
Comparison of the binder amount and compressive strength (28 days) of optimised and non-optimised UHPFRC.

References	Binders (kg/m^3)			Water/ binder ratio	Steel fibre amount (vol.%)	Compressive strength at 28 days (MPa)
	Cement	GGBS	Silica fume			
Yang [6]	950	0	238	0.2	2	190
Kang [9]	860	0	215	0.2	2	198
Hassan [15]	657	418	119	0.17	2	150
Yang [18]	657	430	119	0.15	2	120
Toledo Filho [26]	1011	0	58	0.15	2	160
Corinaldesi [57]	960	0	240	0.16	2.5	155
Habel [58]	1050	0	275	0.14	6	160
UHPC1	875	0	44	0.19	2.5	156
UHPC2	612	0	44	0.19	2.5	142
UHPC3	700	0	44	0.19	2.5	149

The flexural and compressive strength improvement ratios of the UHPC mixes versus the volumetric steel fibres content are illustrated in Figs. 11 and 12, respectively. As indicated in Fig. 11, with an increase of the steel fibres content, a parabolic increase tendency of the flexural strength improvement ratio can be observed. The more fibres are added, the faster the flexural strength improvement ratio grows, which also implies that the addition of steel fibres is more significantly enhancing the flexural strength. Moreover, the difference in the flexural strength improvement ratio between the UHPFRC is small when only 0.5% of steel fibres are added. Nevertheless, with an increase of the steel fibre content, the growth rate of UHPC2 is faster than that of UHPC3 and UHPC1. For instance, with only 0.5% of steel fibres, the flexural strength improvement ratios of UHPC1, UHPC2 and UHPC3 at 28 days are 8.24%, 4.42% and 3.84, which then increase to 84.01%, 129.34% and 96.34, respectively, when 2.5% of steel fibres are included. As can be seen in Fig. 12, with an increase of the steel fibres content, there is a linear increase tendency of the compressive strength improvement ratio in each mixture. Similarly to the results shown in Fig. 11, the difference of compressive strength improvement ratio between the UHPC is not obvious when small amount of steel fibres (around 0.5%) are added. When more steel fibres are included (more than 2%), the increase rate of such value of UHPC2 is much higher than that of UHPC3 and UHPC1.

Hence, it can be summarised that the inclusion of steel fibres can bring considerable enhancement to the strengths of UHPC, especially to the flexural strength. Additionally, the efficiency of additional fibres in UHPC2 is higher and more notable compared to the other groups. This may be due to the low cement content and the inclusion of large quantity of filler materials in UHPC2.

However, it can be noticed that the porosities and the compressive strengths of the designed UHPCs follow the same order:

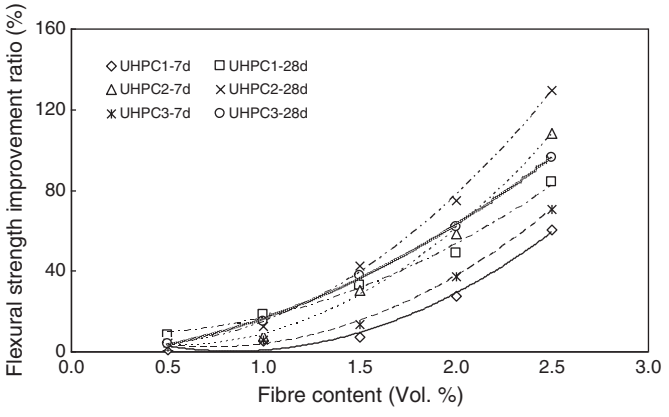

Fig. 11. Flexural strength improvement ratios of UHPFRC at 7 and 28 days as function of steel fibre content.

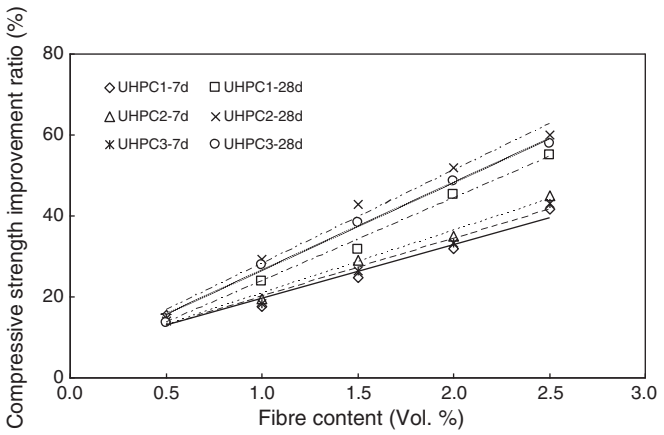

Fig. 12. Compressive strength improvement ratios of UHPFRC at 7 and 28 days as function of steel fibre content.

UHPC1 > UHPC3 > UHPC2, which is not in line with the theory that a larger porosity corresponds to a lower compressive strength. Here, this phenomenon may be attributed to the variation of the cement content in each designed UHPCs. It can be noticed that, based on the modified Andreasen and Andersen packing model, the porosities of all the designed UHPCs are low and similar to each other (as shown in Fig. 7 and 8). Furthermore, the cement amount in UHPC1 is obviously larger than that in UHPC2 and UHPC3, which may cause that more cement particles can hydrate. However, to clearly explain this question and accurately calculate the hydrated cement amount in the designed UHPCs, the cement hydration degree of each sample should be firstly calculated, which will be shown in the following part.

Consequently, it can be concluded that based on the modified Andreasen & Andersen particle packing model, it is possible to produce a UHPFRC with a low binder amount. When utilizing quartz powder to replace about 20% cement, the decrease of flexural and compressive strengths is not obvious. On the other hand, using limestone powder to replace around 30% cement in preparing UHPFRC, the strengths will decrease about 10%, but the efficiency of steel fibres and cement can be significantly enhanced.

3.4. Thermal properties analysis of UHPFRC

The DSC and TG curves of the UHPC pastes after hydrating for 7 and 28 days are presented in Fig. 13 and 14. From the DSC curves, it is apparent that there main peaks exist in the vicinity of 120 °C, 450 °C and 820 °C for all the samples, which should be attributed to the evaporation of free water, decomposition of $Ca(OH)_2$ and decomposition of $CaCO_3$, respectively [52–56]. Normally, there is also a peak at about 576 °C, which is due to the conversion of quartz (SiO_2) present in the sand from α-SiO_2 to β-SiO_2. However, in this study, this peak has not

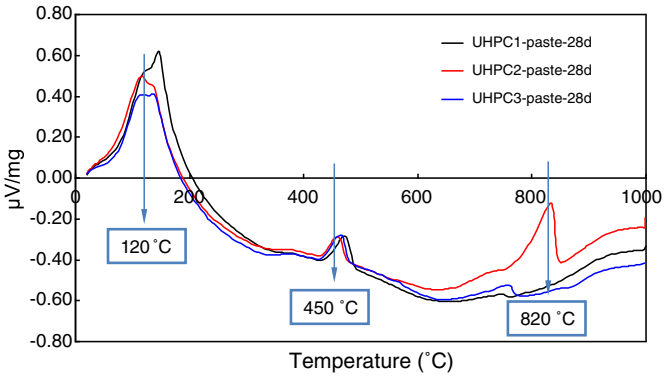

Fig. 13. DSC curves of UHPC pastes after hydrating for 7 and 28 days.

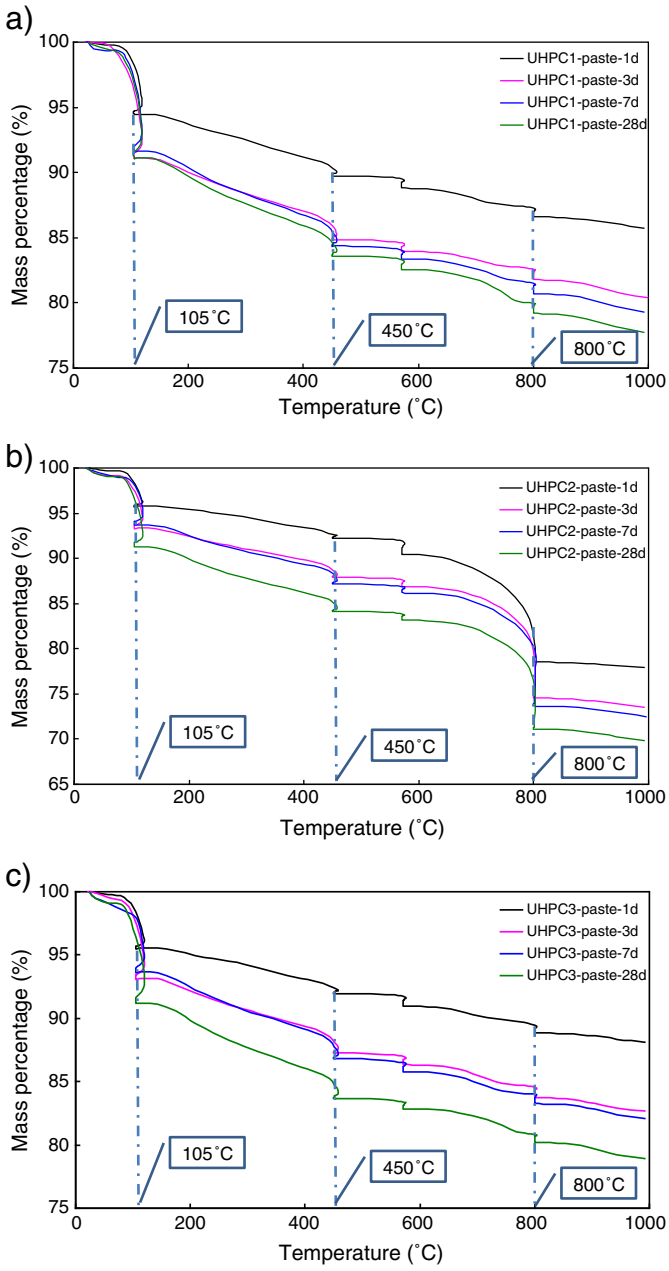

Fig. 14. TG curves of UHPC pastes after hydrating for 1, 3, 7 and 28 days: a) UHPC1, b) UHPC2, c) UHPC3.

been found, which may be attributed to the absence of aggregates in the tested sample and the low content of quartz powder.

Based on the test results shown in Fig. 13, the samples for TG analysis were subjected to isothermal treatment during the test, which was set at 105 °C, 450 °C, 570 °C and 800 °C for 2 h. As can be seen in Fig. 14, the TG curves of all the UHPC pastes show a similar tendency of losing their mass. However, their weight loss rate at each temperature range is different, which means that the amount of the reacted substances in each treatment stage is different. Taking the UHPC2 paste as an example, there is an obvious weight loss at 800 °C, which is caused by the decomposition of $CaCO_3$. In addition, with an increase of the curing time, the weight loss at 800 °C simultaneously increases, which means the hydration of cement is still ongoing, and more $Ca(OH)_2$ is generated and carbonated. Hence, to calculate the cement hydration degree in UHPC paste, the decomposition of $CaCO_3$ (both from limestone powder and from carbonation of $Ca(OH)_2$) must not be ignored.

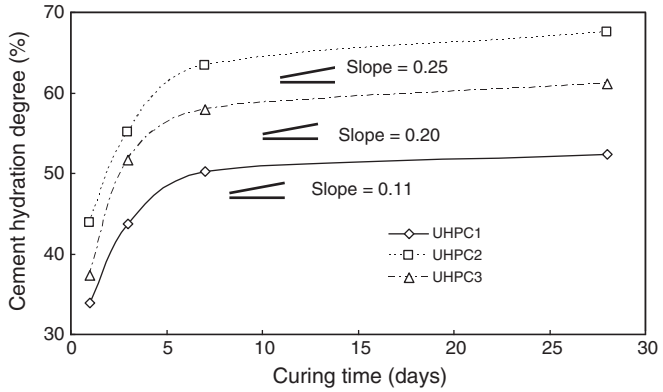

Fig. 15. Cement hydration degrees in each UHPC paste after hydrating for 1, 3, 7 and 28 days.

Here, the hydration degree of the cement in UHPFRC paste after hydrating for 1, 3, 7 and 28 days is computed based on the TG results and Eq. (10). As indicated in Fig. 15, the shapes of the three curves are similar to each other. The shape of these curves can be characterised with a sharp increase before 3 days, followed by a gradual slowing down between 3 and 7 days and a region of a very low increase later. This indicates that the hydration speed of cement in UHPC paste is fast during the first 3 days, then gradually becomes slower and very slow after 7 days. For instance, after curing for 7 days, the hydration degree of cement in UHPC1 is 50.3%, which increases only to 52.4% at 28 days. Furthermore, the cement hydration degree in UHPC2 paste is always the highest, which is followed by UHPC3 and UHPC1, respectively. This phenomenon can be explained by the following two reasons: on one hand, the water/cement ratios of UHPC1, UHPC2 and UHPC3 are 0.23, 0.33 and 0.29, respectively. Hence, after the same curing time, a larger water/cement ratio corresponds to a larger degree of the cement hydration. On the other hand, due to the addition of limestone and quartz powder, the nucleation effect coming from the fine particles may also promote the hydration of cement. Additionally, as shown in Fig. 15, the cement hydration degrees of UHPC1, UHPC2 and UHPC3 at 28 days are 52.4%, 67.6% and 61.1%, respectively. Based on the cement amount in each mixes (in Table 2), it can be calculated that the reacted cement amount (after 28 days) of the designed UHPCs are 458.5 kg/m^3, 413.8 kg/m^3 and 427.9 kg/m^3, respectively. Hence, it is clear that more cement hydrated in UHPC1, compared to the UHPC2 and UHPC3. This can also explain the phenomenon that the compressive strengths of the designed UHPCs follow the same order: UHPC1 > UHPC3 > UHPC2.

In summary, in the mix design and production of UHPFRC, appropriate utilizing filler materials (such as limestone powder and quartz powder in this study) to replace the cement can significantly enhance the cement hydration degree and its service efficiency.

4. Conclusions

This paper presents the mix design and properties assessment for an Ultra-High Performance Fibre Reinforced Concrete (UHPFRC). The design of the concrete mixtures is based on the aim to achieve a densely compacted cementitious matrix, employing the modified Andreasen & Andersen particle packing model. From the presented results the following conclusions are drawn:

- Using the Andreasen & Andersen particle packing model, it is possible to produce a dense and homogeneous skeleton of UHPC using a relatively low binder amount (about 650 kg/m^3). In this study, the maximum compressive and flexural strengths at 28 days of the obtained UHPFRC (with steel fibre 2.5 vol.%) are about 150 MPa and 30 MPa, respectively.
- Due to the low water/binder ratio and relatively large cement content, the degree of hydration is small. Hence, it is reasonable to replace the

unreacted cement with some cheaper filler materials (such as limestone and quartz powder) to enhance the efficiency of the used cement.
- Using fillers (such as limestone and quartz powder) as a cement replacement to produce UHPFRC can significantly improve its workability and enhance the efficiency of steel fibres and binder. Additionally, the utilisation of fillers can also reduce the required amount of micro silica, which is significant for UHPFRC both in economic and environmental aspects.
- The addition of steel fibres can decrease the relative slump flow of UHPFRC and increase its air content in the fresh state and porosity in the hardened state. Nevertheless, an appropriate particle packing and low cement content should be treated as the effective methods to reduce the negative influence of the additional steel fibres.

5. List of symbols

D_{max}	Maximum particle size	μm
D_{min}	Minimum particle size	μm
q	Distribution modulus	
RSS	Sum of the squares of the residuals	
P_{mix}	Composed mix	
P_{tar}	Target curve	
ξ_p	Relative slump flow of fresh concrete	
φ_{air}	Air content of UHPFRC	%
$V_{container}$	Volume of the container	cm^3
V_{solid}	Volume of solid particles in the container	cm^3
V_{liquid}	Volume of liquid in the container	cm^3
M_i	Mass of the fraction i in solid materials	g
ρ_i	Density of the fraction i in solid materials	g/cm^3
M_j	Mass of the fraction j in liquid materials	g
ρ_j	Density of the fraction j in liquid materials	g/cm^3
$\phi_{v,water}$	Water-permeable porosity	%
m_s	Surface dried mass of water saturated sample in air	g
m_w	Mass of water-saturated sample in water	g
m_d	Mass of oven-dry sample	g
M'_{Water}	Mass of non-evaporable water	g
M_{105}	Mass of UHPC paste after heat treatment under 105 °C for 2 h	g
M_{1000}	Mass of UHPC paste after heat treatment under 1000 °C for 2 h	g
M_{CaCO_3}	Mass change of UHPC paste caused by the decomposition of $CaCO_3$	g
β_t	Degree of cement hydration at hydration time t (days)	%
$M_{Water-Full}$	Water requirement of full hydration cement	g
K_t	Strength improvement ratio	%
S_i	Strength of UHPC with fibres (i means the fibres content)	N/mm^2
S_0	Strength of UHPC without fibres	N/mm^2

Acknowledgements

The authors wish to express their gratitude to Dr. Q. Yu for his help, to "BEKAERT" for supplying the steel fibres and to the following sponsors of the Building Materials research group at TU Eindhoven: Rijkswaterstaat Grote Projecten en Onderhoud, Graniet-Import Benelux, Kijlstra Betonmortel, Struyk Verwo, Attero, Enci, Provincie Overijssel, Rijkswaterstaat Zee en Delta—District Noord, Van Gansewinkel Minerals, BTE, Alvon Bouwsystemen, V.d. Bosch Beton, Selor, Twee "R" Recycling, GMB, Schenk Concrete Consultancy, Geochem Research, Icopal, BN International, APP All Remove, Consensor, Eltomation, Knauf Gips, Hess ACC Systems, Kronos and Joma (in chronological order of joining).

References

[1] P. Richard, M. Cheyrezy, Composition of reactive powder concretes, Cem. Concr. Res. 25 (7) (1995) 1501–1511.
[2] P. Rossi, Influence of fibre geometry and matrix maturity on the mechanical performance of ultra-high-performance cement-based composites, Cem. Concr. Compos. 37 (2013) 246–248.
[3] S.H. Park, D.J. Kim, G.S. Ryu, K.T. Koh, Tensile behaviour of Ultra-High Performance Hybrid Fibre Reinforced Concrete, Cem. Concr. Compos. 34 (2012) 172–184.
[4] A.S. El-Dieb, Mechanical, durability and microstructural characteristics of ultra-high-strength self-compacting concrete incorporating steel fibres, Mater. Des. 30 (2009) 4286–4292.
[5] B.A. Tayeh, B.H. Abu Bakar, M.A. Megat Johari, Y.L. Voo, Mechanical and permeability properties of the interface between normal concrete substrate and ultra-high performance fibre concrete overlay, Constr. Build Mater. 36 (2012) 538–548.
[6] A.M.T. Hassan, S.W. Jones, G.H. Mahmud, Experimental test methods to determine the uniaxial tensile and compressive behaviour of ultra-high performance fibre reinforced concrete (UHPFRC), Constr. Build Mater. 37 (2012) 874–882.
[7] N.V. Tuan, G. Ye, K. Breugel, O. Copuroglu, Hydration and microstructure of ultra-high performance concrete incorporating rice husk ash, Cem. Concr. Res. 41 (2011) 1104–1111.
[8] N.V. Tuan, G. Ye, K. Breugel, A.L.A. Fraaij, B.D. Dai, The study of using rice husk ash to produce ultra-high performance concrete, Constr. Build Mater. 25 (2011) 2030–2035.
[9] S.L. Yang, S.G. Millard, M.N. Soutsos, S.J. Barnett, T.T. Le, Influence of aggregate and curing regime on the mechanical properties of ultra-high performance fibre reinforced concrete (UHPFRC), Constr. Build Mater. 23 (2009) 2291–2298.
[10] UNSTATS, Greenhouse gas emissions by sector (absolute values), United Nation Statistical Division, Springer, 2010.
[11] P. Friedlingstein, R.A. Houghton, G. Marland, J. Hackler, T.A. Boden, T.J. Conway, et al., Uptake on CO_2 emissions, Nat. Geosci. 3 (2010) 811–812.
[12] P. Capros, N. Kouvaritakis, L. Mantzos, Economic evaluation of sectorial emission reduction objectives for climate change top-down analysis of greenhouse gas emission possibilities in the EU, Contribution to a study for DG environment. European commission 2001.
[13] G. Habert, E. Denarié, A. Šajna, P. Rossi, Lowering the global warming impact of bridge rehabilitations by using Ultra High Performance Fibre Reinforced Concretes, Cem. Concr. Comput. 38 (2013) 1–11.
[14] E. Denarié, E. Brühwiler, Strain Hardening Ultra-high Performance Fibre Reinforced Concrete: Deformability versus Strength Optimization, Int. J. Restauration Build. Monuments 17 (6) (2011) 397–410(Aedificatio).
[15] E. Brühwiler, E. Denarié, Rehabilitation of concrete structures using ultra-high performance fibre reinforced concrete, Proceedings, UHPC-2008: the second international symposium on ultra-high performance concrete, March 05–07, 2008, Kassel, Germany, 2008.
[16] R. Bornemann, M. Schmidt, The role of powders in concrete, Proceedings 6th international symposium on utilisation of high strength/high performance concrete, Leipzig, 2, 2002, pp. 863–872.
[17] H.J.H. Brouwers, H.J. Radix, Self compacting concrete: theoretical and experimental study, Cem. Concr. Res. 35 (2005) 2116–2136.
[18] G. Hüsken, A multifunctional design approach for sustainable concrete with application to concrete mass products, PhD thesis Eindhoven University of Technology, Eindhoven, the Netherlands, 2010.
[19] M. Hunger, An integral design concept for ecological self-compacting concrete, PhD thesis Eindhoven University of Technology, Eindhoven, the Netherlands, 2010.
[20] R.D. Toledo Filho, E.A.B. Koenders, S. Formagini, E.M.R. Fairbairn, Performance assessment of Ultra-High Performance Fibre Reinforced Cementitious Composites in view of sustainability, Mater. Des. 36 (2012) 880–888.
[21] F. De Larrard, T. Sedran, Optimization of ultra-high-performance concrete by the use of a packing model, Cem. Concr. Res. 24 (1994) 997–1009.
[22] F. De Larrard, T. Sedran, Mixture-proportioning of high-performance concrete, Cem. Concr. Res. 32 (2002) 1699–1704.
[23] U. Stark, A. Mueller, Optimization of packing density of aggregates, Proceedings of the Second International Symposium on Ultra-High Performance Concrete. Kassel, Germany, March 05–07, 2008.
[24] S.A.A.M. Fennis, J.C. Walraven, J.A. den Uijl, The use of particle packing models to design ecological concrete, Heron 54 (2009) 185–204.
[25] W.B. Fuller, S.E. Thompson, The laws of proportioning concrete, Trans. Am. Soc. Civ. Eng. 33 (1907) 222–298.
[26] A.H.M. Andreasen, J. Andersen, Über die Beziehungen zwischen Kornabstufungen und Zwischenraum in Produkten aus losen Körnern (mit einigen Experimenten), Kolloid Z. 50 (1930) 217–228(In German).
[27] J.E. Funk, D.R. Dinger, Predictive Process Control of Crowded Particulate Suspensions, Applied to Ceramic Manufacturing, Kluwer Academic Publishers, Boston, the United States, 1994..
[28] Q.L. Yu, P. Spiesz, H.J.H. Brouwers, Development of cement-based lightweight composites—Part 1: Mix design methodology and hardened properties, Cem. Concr. Comput. 44 (2013) 17–29.
[29] P. Spiesz, Q.L. Yu, H.J.H. Brouwers, Development of cement-based lightweight composites—Part 2: Durability related properties, Cem. Concr. Comput. 44 (2013) 30–40.
[30] G. Hüsken, H.J.H. Brouwers, A new mix design concept for each-moist concrete: a theoretical and experimental study, Cem. Concr. Res. 38 (2008) 1249–1259.
[31] H.J.H. Brouwers, Particle-size distribution and packing fraction of geometric random packings, Phys. Rev. E 74 (2006) 031309-1–031309-14.
[32] S. Grünewald, Performance-based design of self-compacting fibre reinforced concrete, Delft University of Technology, Delft, the Netherlands, 2004.
[33] I.H. Yang, C. Joh, B.S. Kim, Structural behaviour of ultra-high performance concrete beams subjected to bending, Eng. Struct. 32 (2010) 3478–3487.

[34] BS-EN-1015-3, Methods of test for mortar for masonry—Part 3: Determination of consistence of fresh mortar (by flow table), British Standards Institution-BSI and CEN European Committee for Standardization 2007.
[35] H. Okamura, K. Ozawa, Mix-design for self-compacting concrete, Concr. Libr. JSCE 25 (1995) 107–120.
[36] BS-EN-196-1, Methods of testing cement—Part 1: Determination of strength, British Standards Institution-BSI and CEN European Committee for Standardization 2005.
[37] M.d Safiuddin, N. Hearn, Comparison of ASTM saturation techniques for measuring the permeable porosity of concrete, Cem. Concr. Res. 35 (2005) 1008–1013.
[38] NT Build 492, Concrete, mortar and cement-based repair materials: chloride migration coefficient from non-steady-state migration experiments, Nordtest method 1999. (Finland).
[39] ASTM C1202, Standard Test Method for Electrical Indication of Concrete's Ability to Resist Chloride Ion Penetration, Annual Book of ASTM Standards, vol. 04.02, American Society for Testing and Materials, Philadelphia, 2005. (July).
[40] D. Bentz, X. Feng, C. Haecker, P. Stutzman, Analysis of CCRL proficiency cements 135 and 136 using CEMHYD3D, NIST Internal Report 6545, 2000. (August).
[41] I. Pane, W. Hansen, Investigation of blended cement hydration by isothermal calorimetry and thermal analysis, Cem. Concr. Res. 35 (2005) 1155–1164.
[42] Edgington J., Hannant D.J., Williams R.I.T., Steel Fibre Reinforced Concrete, Fibre Reinforced Materials, The Construction Press, Lancaster, England, 112–128.
[43] B. Madani, M. Zoubir, B. Tayeb, Effect of limestone fillers the physic-mechanical properties of limestone concrete, Phys. Process. 21 (2011) 28–34.
[44] B.B. Violeta, SCC mixes with poorly graded aggregate and high volume of limestone filler, Cem. Concr. Res. 33 (9) (2003) 1279–1286.
[45] G. Mehmet, G. Erhan, E.K. Mustafa, B. Veysel, M. Kasım, Fresh and hardened characteristics of self compacting concretes made with combined use of marble powder, limestone filler, and fly ash, Constr. Build. Mater. 37 (2012) 160–170.
[46] E. Tazawa, S. Miyazawa, Effect of constituents and curing conditions on autogenous shrinkage of concrete, in: E. Tazawa (Ed.), Autogenous Shrinkage of Concrete, Taylor & Francis, 1999, pp. 269–280.
[47] Y. Zhang, W. Sun, S. Liu, C. Jiao, J. Lai, Preparation of C200 green reactive powder concrete and its static–dynamic behaviours, Cem. Concr. Comput. 30 (2008) 831–838.
[48] J. Romualdi, J. Mandel, Tensile strength of concrete affected by uniformly distributed and closely spaced short lengths of wire reinforcement, J. Am. Concr. Inst. 61 (6) (1964) 657–671.
[49] P. Rossi, P. Acker, Y. Malier, Effect of steel fibres at two stages: the material and the structure, Mater. Struct. 20 (1987) 436–439.
[50] W. Sun, J.A. Mandel, S. Said, Study of the interface strength of steel fibre reinforced cement based composites, ACI Mater. J. 83 (1986) 597–605.
[51] X.C. Pu, Super High Strength and High Performance Concrete, Chongqing University Press, China, 2004.
[52] C. Alonso, L. Fernandez, Dehydration and rehydration processes of cement paste exposed to high temperature environments, J. Mater. Sci. 39 (9) (2004) 3015–3024.
[53] L. Alarcon-Ruiz, G. Platret, E. Massieu, A. Ehrlacher, The use of thermal analysis in assessing the effect of temperature on a cement paste, Cem. Concr. Res. 35 (3) (2005) 609–613.
[54] M. Castellote, C. Alonso, C. Andrade, X. Turrillas, J. Campo, Composition and microstructural changes of cement pastes upon heating, as studied by neutron diffraction, Cem. Concr. Res. 34 (9) (2004) 1633–1644.
[55] P.E. Grattan-Bellew, Microstructural investigation of deteriorated Portland cement concretes, Constr. Build. Mater. 10 (1) (1996) 3–16.
[56] S.K. Handoo, S. Agarwal, S.K. Agarwal, Physicochemical, mineralogical, and morphological characteristics of concrete exposed to elevated temperatures, Cem. Concr. Res. 32 (7) (2002) 1009–1018.
[57] V. Corinaldesi, G. Moriconi, Mechanical and thermal evaluation of Ultra-High Performance Fiber Reinforced Concretes for engineering applications, Constr. Build. Mater. 26 (2012) 289–294.
[58] K. Habel, M. Viviani, E. Denarié, E. Brühwiler, Development of the mechanical properties of an Ultra-High Performance Fiber Reinforced Concrete (UHPFRC), Cem. Concr. Res. 36 (2006) 1362–1370.